Indian Journal of Pure & Applied Physics
Vol. 55, January 2017, pp. 25-42

Vibrational spectroscopy analysis and molecular conformational stability of N-((3-methyl-1-(phenylsulfonyl)-1H-indol-2-yl)methyl) acetamide

R Srinivasaraghavan[a], S Seshadri[b]* & T Gnanasambandan[c]

[a]Department of Physics, SCSVMV University, Kanchipuram 631 561, India
[b]Department of Physics, Dr. Ambedkar Government College, Vyasarpadi, Chennai 600 039, India
[c]Department of Physics, Pallavan college of Engineering, Kanchipuram 631 502, India

Received 19 November 2015; revised 14 July 2016; accepted 5 December 2016

The FTIR and FT Raman vibrational analysis and the fundamental modes of N-((3-methyl-1-(phenylsulfonyl)-1H-indol-2-yl)methyl) acetamide [N3MP2MA] have been carried out. On the basis of quantum chemical calculations in B3LYP/6-31G(d,p) and B3LYP/6-311++G(d,p) levels the geometric parameters, vibrational analysis have been obtained. The experimental vibrational data have been compared with the wavenumbers derived theoretically. The intramolecular contacts have been interpreted using natural bond orbital (NBO) and natural localized molecular orbital (NLMO) analysis. Important non-linear properties such as electric dipole moment and first hyperpolarizability of N3MP2MA have been computed using B3LYP quantum chemical calculations. Finally, the HOMO-LUMO energy gap and the Mulliken population analysis on atomic charges of the title compound has been calculated.

Keywords: N3MP2MA, Potential energy distribution, Natural bond orbital, Natural localized molecular orbital, MEP

1 Introduction

The title compound $C_{18}H_{18}N_2O_3S_2$ that has a phenylsulfonyl ring and phenylthio ring make dihedral angles with an indole unit. Indole derivatives are found to exhibit antibacterial, antifungal[1] and anti-tumour activities[2]. Some of the indole alkaloids extracted from plants possess interesting cytotoxic, anti-tumour or antiparasitic properties[3,4]. Pyrido [1,2-*a*] indole derivatives have been identified as potent inhibitors of human immune-deficiency virus type 1, and 5-chloro-3-(phenylsulfonyl) indole-2-carboxamide is reported[5] to be a highly potent non-nucleoside inhibitor of HIV-1 reverse transcriptase[6]. The interaction of phenylsulfonylindole with calf thymus DNA has also been studied by spectroscopic methods[7]. The XRD details and structural identification work of the title compound was done by Thenmozhi *et al.*[8] and no further work had been carried out so far. With this background and in order to obtain detailed information on molecular conformations in the solid state, vibrational spectroscopic investigation and assignments using DFT techniques and electronic transitions of N-((3-methyl-1-(phenylsulfonyl)-1H-indol-2-yl) methyl)acetamide (N3MP2MA) were reported in this study. In the ground state, theoretical geometrical parameters, IR and Raman spectra, HOMO and LUMO energies of title molecule were calculated by using Gaussian 03W program. Detailed interpretations of the vibrational spectra of the N3MP2MA was made on the basis of the calculated potential energy distribution (PED). The experimental results (IR and Raman spectra) were supported by the computed results, comparing with experimental characterization data; vibrational wavenumbers are in fairly good agreement with the experimental results. The redistribution of electron density (ED) in various bonding, antibonding orbitals and E(2) energies have been calculated by natural bond orbital (NBO)/natural localized molecular orbital (NLMO) analysis to give clear evidence of stabilization originating from the hyper conjugation of various intra-molecular interactions. By analyzing the density of states, the molecular orbital compositions and their contributions to the chemical bonding were studied. The study of HOMO, LUMO analysis was used to elucidate information regarding charge transfer within the molecule. Moreover, the Mulliken population analyses of the title compound was calculated and the results were reported. The experimental and theoretical results supported each other and the calculations are valuable for providing a reliable insight into the vibrational spectra and molecular properties.

*Corresponding author (E-mail: sri_sesha@yahoo.com)

2 Experimental

The compound N-((3-methyl-1-(phenylsulfonyl)-1H-indol-2-yl)methyl)acetamide [N3MP2MA] was a synthesized one and used as such to record the FTIR and FT Raman spectra. The FTIR spectrum of the compound is recorded in the region 4000 – 400 cm^{-1} in evacuation mode on Bruker IFS 66V spectrophotometer using KBr pellet technique (solid phase) with 4.0 cm^{-1} resolutions. The FT-Raman spectrum of the compound is recorded in the same instrument with FRA 106 Raman module equipped with Nd: YAG laser source operating at 1.064μm line widths with 200 mW power. The spectra are recorded in the range of 3500–100 cm^{-1} with scanning speed of 30 cm^{-1} min^{-1} of spectral width 2 cm^{-1}. The wavenumbers of all sharp bands are accurate to ±1 cm^{-1}. The spectral measurements were carried out at Sophisticated Analytical Instrumentation Facility, IIT Chennai, India.

3 Computational Details

The primary task for the computational work was to determine the optimized geometry of the compound using Gaussian 03W software[9]. It was found that the calculations could achieve convergence more rapidly if the input data were closer to the experimental values of the minimal energy points of the molecules. Therefore the geometry optimization was started from the X-ray experimental atomic positions. It is more popular that in quantum chemical literation that the hybrid B3LYP method based on Becke's three parameter functional of DFT yields a good description of harmonic vibrational wavenumbers for molecules[10]. The geometry optimization was carried out using the initial geometry generated from standard geometrical parameters at B3LYP method with flexible basis sets 6-31G(d, p) and 6-311++G(d, p) level. The Cartesian representation of the theoretical force constants were computed at the fully optimized geometry. Harmonic vibrational wavenumbers were calculated using analytic second derivatives to confirm the convergence to minima in the potential surface. The calculated frequencies are scaled according to the work of Rauhut and Pulay[11,12] a scaling factor of 0.9631 for B3LYP/6-31G(d, p) and 0.967 for B3LYP/6-311++G(d, p).

PED calculations which shows the relative contribution of the redundant internal coordinates to each normal vibrational mode of the molecule, and thus enable us numerically to describe the character of each mode were carried out by SQM method using the output files generated at the end of the calculations. The selective scaling procedure was adopted according to SQM procedure in the natural internal coordinate representation [13,14] the transformation of force field; subsequent normal coordinates analysis and calculation of the potential energy distribution (PED) were done on a PC with the MOLVIB program (version V7.0-G77) written by Sundius[15-17]. By the use of GAUSSVIEW molecular visualization program[18] along with available related molecules; the vibrational frequency assignments were made by their PED with a high degree of confidence. The PED elements provide a measure of each internal coordinate's contribution to the normal coordinates.

4 Results and Discussion

4.1 Molecular geometry

The most optimized geometry was studied and the energies were carried out for N3MP2MA, using B3LYP/6-311++G(d,p) method for various possible conformational analysis. There are about twelve conformers obtained for N-((3-methyl-1-(phenylsulfonyl)-1H-indol-2-yl)methyl)acetamide [N3MP2MA]. The computationally predicted structures for various possible conformers of N3MP2MA are shown in Fig. 1. The total energies obtained for these conformers are listed in Table 1. It is clear in Table 1, the structure optimizations have shown that the conformer C_2 have produced the global minimum energy of 373.4454KJ/Cal. Therefore, C_2 form is the most stable conformer than the other conformers. The optimized molecular structure with the numbering of atoms of the N3MP2MA is shown in Fig. 2. The most optimized structural parameters of N3MP2MA calculated by DFT-B3LYP level with the 6-31G(d,p) and 6-311++G(d,p) basis set are listed in the Table 2 in accordance with the atom numbering scheme given in Fig. 2. The optimized molecular structure of N3MP2MA belongs to C_1 point group symmetry. Table 2 compares the calculated bond lengths and angles for N3MP2MA with those experimentally available from literature value[8]. From the theoretical values, we can find that most of the optimized bond angles are slightly differ from the experimental values, due to the theoretical calculations belong to isolated molecules in gaseous phase and the experimental results belong to molecules in solid state. The theoretical values for the N3MP2MA molecule were compared with the experimental values by means of the root mean square deviation values. Comparing the B3LYP/6-31G(d,p) and B3LYP/6-311++G(d,p) methods most of the bond

lengths and bond angles are the same in both the methods. The inclusion of diffusion and polarization functions is important to have a better agreement with experimental geometry.

4.2 Vibrational assignments

The experimental and theoretical Infrared and Raman spectra of N3MP2MA are shown in Figs 3 and 4, respectively. The molecule N3MP2MA consists of 42 atoms and expected to have 120 normal modes of vibrations of the same A species under C_1 symmetry. These modes are found to be IR and Raman active suggesting that the molecule possesses a non-Centro symmetric structure, which recommends the title

Table 1 — Total energies of different conformations of N3MP2MA calculated at the B3LYP/6-311++G(d,p) level of theory

S No	Conformers	Energy (kJ/Mol)
1	C_1	471.5669
2	C_2	373.4454
3	C_3	404.4637
4	C_4	552.4326
5	C_5	446.5727
6	C_6	2114.8229
7	C_7	729.1603
8	C_8	2016.6872
9	C_9	549.5050
10	C_{10}	486.4546

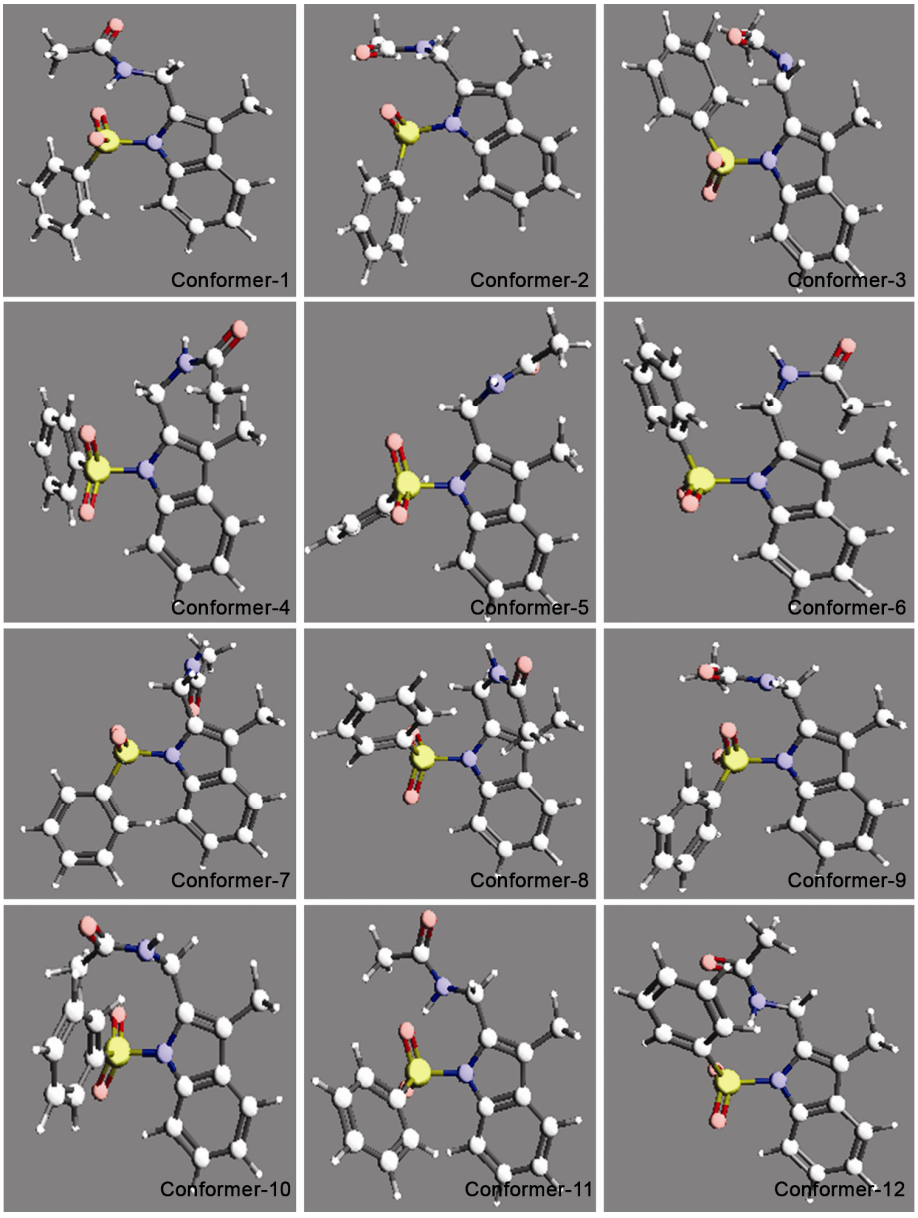

Fig. 1 — Various possible conformers of N3MP2MA

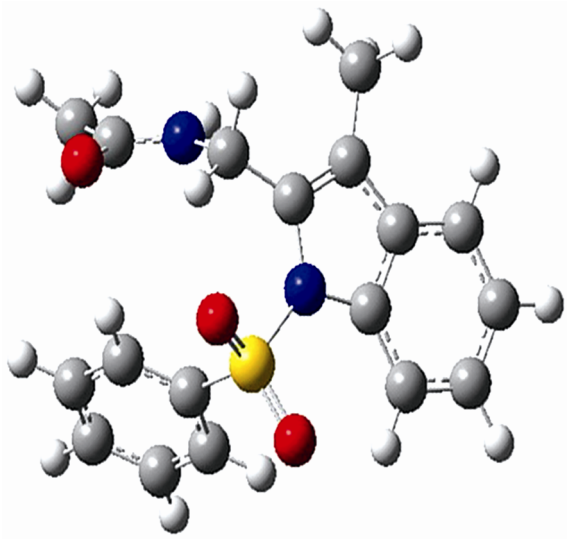

Fig.2 — Structure of N3MP2MA

compound for nonlinear optical applications. The harmonic vibrational modes calculated for N3MP2MA at B3LYP level using the 6-31G(d,p) and 6-311++G(d,p) basis set along with potential energy distribution have been summarized in Table 3. The observed FTIR and FT Raman bands for various modes of vibrations of N3MP2MA are assigned and are presented in the Table 3 along with the DFT data. The force fields thus determined were used to calculate the vibrational potential energy distribution (PED) using the latest version of MOLVIB program[15-17]. Calculations were made for a free molecule in vacuum, while experiments were performed in solid phase. Furthermore the anharmonicity is neglected in real system for calculated vibrations and because of the low IR and Raman intensity of some modes, it is difficult to observe them in the IR and Raman spectra. Thus, there are disagreements between calculated and observed vibration wavenumbers. These discrepancies were corrected either by computing anharmonic corrections explicitly or by introducing a scaled field or by directly scaling the calculated wavenumbers with a proper factor. Considering the systematic errors, the calculated wavenumbers are calibrated with the scaling factors of 0.9631 for B3LYP/6-31G(d, p) and 0.967 for B3LYP/6-311++G(d, p). In order to reproduce the calculated frequencies, the scale factors were refined and optimized via a least squares refinement algorithm.

4.2.1 C-H Vibrations

The existence of one or more aromatic rings in a structure is normally determined from C-H and C=C-C ring related vibrations. In the aromatic compounds, the carbon–hydrogen stretching vibrations[19] normally occur at 3250–3000 cm^{-1}. Heterocyclic compound C-H vibration absorption bands are usually weak; in many cases it is too weak for detection. The bands due to C–H in-plane bending vibrations interact somewhat with C–C stretching vibrations is observed as a number of bands in the region 1450–1100 cm^{-1}. The C–H out-of-plane bending vibrations[19,20] occur in the region 900–667 cm^{-1}. In this region the vibrations are not found to be affected due to the nature and position of the substituent[21]. In the present work, the bands observed at 3103 cm^{-1}, 3079 cm^{-1}, 3067 cm^{-1}, 3056 cm^{-1} and 3025 cm^{-1}, 2987 cm^{-1}, 2973 cm^{-1} in the N3MP2MA compound have been assigned to C-H stretching vibration. Apart from the mentioned values other vibrations in the same range are assigned to C-H asymmetric and symmetric vibrations respectively. The C-H bending vibrations appear at two distinct regions 1480 - 1300 cm^{-1} and 1100 – 900 cm^{-1}, due to in plane and out of plane bending vibrations respectively[22,23]. The band position observed at 1460 cm^{-1} and 1092 cm^{-1} in experimental spectrum of N3MP2MA are assigned to C-H in plane and out of plane bending vibrations. The wavenumbers calculated through DFT techniques are in good agreement with the experimental data.

4.2.2 C-N vibrations

Because of the mixing of several bands, the identification of C-N stretching vibration is a very difficult task in this region. Silverstein assigned C-N stretching absorption in the region 1382 – 1266 cm^{-1}. In the present work, the FT Raman band observed at 1310 cm^{-1} in N3MP2MA has been designated to the C-N stretching mode of vibration. These assignments are made in accordance with the assignment proposed by Bienko, Michalska *et al.*[24]. The C-N stretching band assigned at 1319 cm^{-1} in 2,6-dibromo-4-nitroaniline by Krishna Kumar[25], Raja *et al.*[26] have identified the FTIR band at 1342 cm^{-1} due to C-N in theophylline. Gunasekaran *et al.*[27] have observed the C-N stretching band at 1312cm^{-1} in benzocaine. The calculated value at 1301 cm^{-1} of N3MP2MA is in excellent agreement with the observed value for the corresponding mode of vibration.

4.2.3 C-C vibrations

The C-C aromatic stretching vibration gives rise to characteristic bands in both the observed IR and Raman spectra, covering the spectral range from 1600 – 1400 cm^{-1}. The IR bands located at 1460, 1448, 1435 cm^{-1} and 1329 cm^{-1}; the Raman bands

Table 2 — Molecular parameters of N3MP2MA

Molecular parameter (Å)	Experimental	6-31G(d,p)	6-311++G(d,p)
C_1-C_2	1.383	1.396	1.391
C_1-O_3	1.227	1.229	1.228
C_1-N_4	1.422	1.393	1.415
C_2-H_{25}	0.930	1.093	0.992
C_2-H_{26}	0.930	1.093	0.992
C_2-H_{27}	0.930	1.093	0.992
N_4-C_5	1.433	1.428	1.426
N_4-H_{28}	0.866	1.009	0.924
C_5-C_7	1.397	1.413	1.408
C_5-H_{29}	0.930	1.086	0.988
C_5-H_{30}	0.930	1.097	0.988
N_6-C_7	1.396	1.419	1.412
N_6-C_{14}	1.396	1.413	1.412
C_7-C_8	1.354	1.367	1.363
C_8-C_9	1.440	1.438	1.445
C_8-C_{24}	1.493	1.483	1.489
C_9-C_{10}	1.392	1.401	1.393
C_9-C_{14}	1.392	1.415	1.397
C_{10}-C_{11}	1.388	1.387	1.390
C_{10}-H_{31}	0.930	1.085	0.992
C_{11}-C_{12}	1.392	1.407	1.402
C_{11}-H_{32}	0.930	1.086	0.992
C_{12}-C_{13}	1.392	1.391	1.390
C_{12}-H_{33}	0.980	1.086	0.992
C_{13}-C_{14}	1.384	1.401	1.402
C_{13}-H_{34}	0.980	1.081	0.992
N_6-S_{15}	1.669	1.741	1.723
S_{15}-O_{16}	1.422	1.429	1.426
S_{15}-O_{17}	1.422	1.428	1.425
S_{15}-C_{18}	1.743	1.790	1.746
C_{18}-C_{19}	1.392	1.397	1.395
C_{18}-C_{23}	1.392	1.397	1.392
C_{19}-C_{20}	1.388	1.394	1.390
C_{19}-H_{35}	0.980	1.083	1.105
C_{20}-C_{21}	1.388	1.397	1.397
C_{20}-H_{36}	0.980	1.085	0.992
C_{21}-C_{22}	1.388	1.396	1.394
C_{21}-H_{37}	0.960	1.086	0.992
C_{22}-C_{23}	1.386	1.395	1.394
C_{22}-H_{38}	0.960	1.085	0.992
C_{23}-H_{39}	0.960	1.086	0.992
C_{24}-H_{40}	0.980	1.083	0.992
C_{24}-H_{41}	0.980	1.083	0.992
C_{24}-H_{42}	0.980	1.083	0.992
Bond angle (°)			
C_2-C_1-O_3	121.800	121.300	121.500
C_2-C_1-N_4	110.600	113.300	113.200
C_1-C_2-H_{25}	109.500	111.900	110.300

(*contd.*)

Table 2 — Molecular parameters of N3MP2MA (*contd.*)

Molecular parameter (Å)	Experimental	6-31G(d,p)	6-311++G(d,p)
C_1-C_2-H_{26}	109.500	108.600	110.600
C_1-C_2-H_{27}	109.500	108.700	108.700
O_3-C_1-N_4	121.100	121.400	121.300
C_1-N_4-C_5	122.020	123.300	122.700
C_1-N_4-H_{28}	118.080	119.100	118.300
H_{25}-C_2-H_{26}	109.500	109.000	109.100
H_{25}-C_2-H_{27}	109.500	109.100	109.000
H_{26}-C_2-H_{27}	109.500	109.700	109.100
C_5-N_4-H_{28}	118.080	117.500	117.300
N_4-C_5-C_7	117.000	115.800	116.100
N_4-C_5-H_{29}	107.400	107.400	107.400
N_4-C_5-H_{30}	107.400	107.900	107.300
C_7-C_5-H_{29}	109.500	110.000	109.400
C_7-C_5-H_{30}	109.500	110.000	109.300
C_5-C_7-N_6	126.500	126.900	126.900
C_5-C_7-C_8	126.500	126.300	126.500
H_{29}-C_5-H_{30}	109.500	109.500	109.700
C_7-N_6-C_{14}	107.600	107.900	107.400
N_6-C_7-C_8	110.600	110.800	110.500
N_6-C_{14}-C_9	110.600	110.500	110.400
N_6-C_{14}-C_{13}	129.700	130.700	130.200
C_7-C_8-C_9	112.300	110.700	111.600
C_7-C_8-C_{24}	113.800	115.400	112.800
C_9-C_8-C_{24}	112.900	112.900	112.900
C_8-C_9-C_{10}	123.300	123.200	123.500
C_8-C_9-C_{14}	115.900	116.100	116.100
C_8-C_{24}-H_{40}	111.400	112.592	111.865
C_8-C_{24}-H_{41}	110.900	112.043	111.872
C_8-C_{24}-H_{42}	112.300	112.686	111.915
C_{10}-C_9-C_{14}	119.400	120.700	120.400
C_9-C_{10}-C_{11}	117.100	118.500	118.600
C_9-C_{10}-H_{31}	119.400	119.800	119.400
C_9-C_{14}-C_{13}	119.100	119.800	119.400
C_{11}-C_{10}-H_{31}	120.500	121.700	121.000
C_{10}-C_{11}-C_{12}	120.500	120.500	121.000
C_{10}-C_{11}-H_{32}	119.400	119.900	119.700
C_{12}-C_{11}-H_{32}	119.400	119.600	119.300
C_{11}-C_{12}-C_{13}	121.900	121.900	121.800
C_{11}-C_{12}-H_{33}	119.400	119.400	119.200
C_{13}-C_{12}-H_{33}	119.000	118.700	119.000
C_{12}-C_{13}-C_{14}	119.000	117.700	117.900
C_{12}-C_{13}-H_{34}	122.000	121.800	121.700
C_{14}-C_{13}-H_{34}	122.000	121.500	121.400
C_7-N_6-S_{15}	122.020	122.363	122.135
C_{14}-N_6-S_{15}	127.030	127.758	127.282
O_{16}-S_{15}-O_{17}	120.110	120.300	120.100
O_{16}-S_{15}-C_{18}	108.500	108.600	108.300
O_{17}-S_{15}-C_{18}	108.500	108.600	108.500

(*contd.*)

Table 2 — Molecular parameters of N3MP2MA (*contd.*)

Molecular parameter (Å)	Experimental	6-31G(d,p)	6-311++G(d,p)
S_{15}-C_{18}-C_{19}	118.700	118.700	118.600
S_{15}-C_{18}-C_{23}	120.300	119.800	120.300
C_{19}-C_{18}-C_{23}	120.700	121.200	120.400
C_{18}-C_{19}-C_{20}	120.400	119.900	120.000
C_{18}-C_{19}-H_{35}	119.800	120.200	119.900
C_{18}-C_{23}-C_{22}	118.300	118.300	118.500
C_{18}-C_{23}-H_{39}	120.700	121.600	120.900
C_{20}-C_{19}-H_{35}	120.700	121.100	120.900
C_{19}-C_{20}-C_{21}	120.400	120.100	120.600
C_{19}-C_{20}-H_{36}	119.600	119.600	120.000
C_{21}-C_{20}-H_{36}	119.600	120.300	120.100
C_{20}-C_{21}-C_{22}	120.400	120.400	120.400
C_{20}-C_{21}-H_{37}	119.600	119.800	119.600
C_{22}-C_{21}-H_{37}	119.600	119.900	119.700
C_{21}-C_{22}-C_{23}	120.700	120.500	120.500
C_{21}-C_{22}-H_{38}	120.000	120.500	120.500
C_{23}-C_{22}-H_{38}	120.000	119.100	119.500
C_{22}-C_{23}-H_{39}	120.000	120.200	119.800
H_{40}-C_{24}-H_{41}	106.900	107.112	107.006
H_{40}-C_{24}-H_{42}	107.700	107.261	107.397
H_{41}-C_{24}-H_{42}	107.500	107.197	107.365

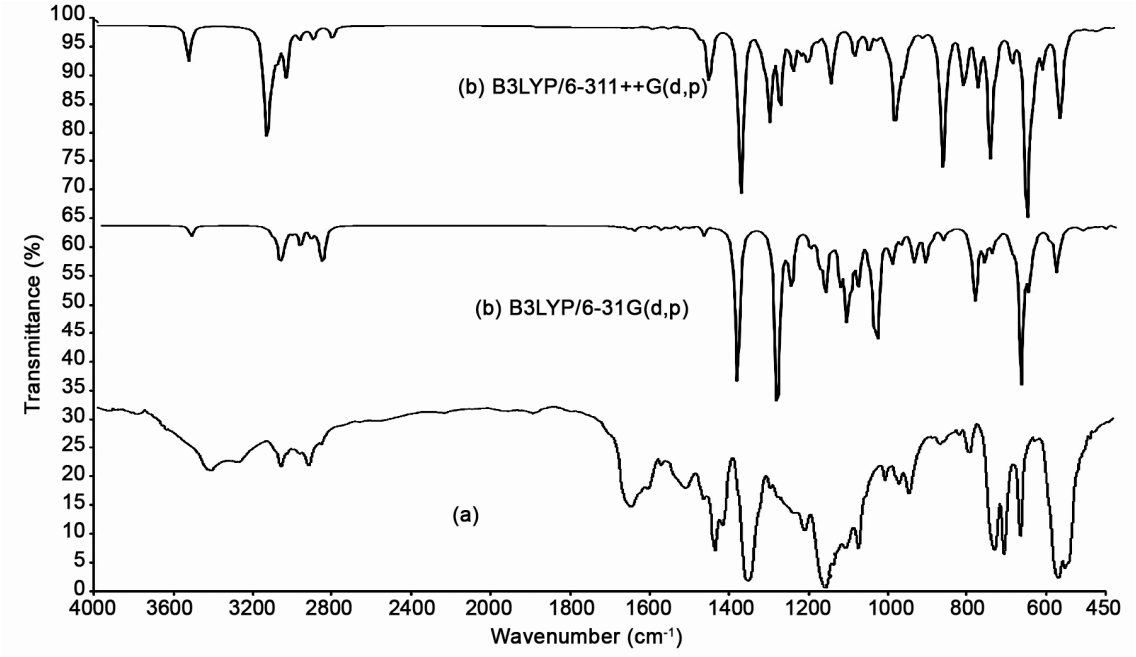

Fig. 3 — Comparative (a) Experimental and (b) Theoretical IR spectra of N3MP2MA

centered at 1460, 1448, 1435 and 1329 cm^{-1} have been assigned to C-C stretching vibrations. Of these bands, 1448 cm^{-1} have appeared characteristically strong in the IR and Raman spectra. The calculated bands at B3LYP level in the same region are in excellent agreement with experimental observations of both in FTIR and FT Raman spectra of N3MP2MA[28-30]. The ring in plane vibration has given rise to weak bands across the low wavenumber region, that is to say, below 1000 cm^{-1}. The bands at 830 cm^{-1} and at 966cm^{-1} have been assigned to C-C in plane bending vibrations. As it can be seen from

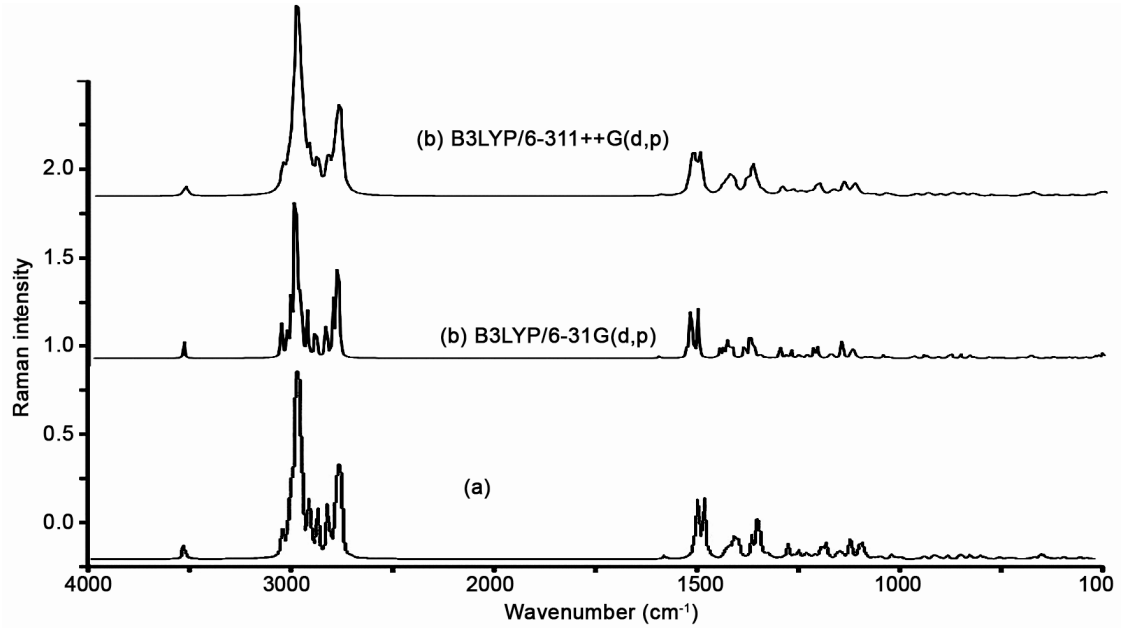

Fig. 4 — Comparative (a) Experimental and (b) Theoretical Raman spectra of N3MP2MA

Table 3 — Vibrational assignments of N3MP2MA using B3LYP/ 6-31 G(d,p) and B3LYP/6-311++G(d,p)

νIR cm^{-1}	ν Raman cm^{-1}	B3LYP/6-31 G(d,p)			B3LYP/6-311++ G(d,p)			Assignments PED %
		ν cm^{-1}	IR intensity	Raman activity	ν cm^{-1}	IR intensity	Raman activity	
		14	0.3972	3.4888	15	1.7185	10.9038	τ ring (32)
		22	0.336	8.1098	22	0.7496	7.6677	β ring (14)
		35	0.9932	4.6801	33	3.2264	0.8863	β ring (27)
		39	1.847	4.0903	39	1.5522	7.1128	τCN (59)
		49	3.7678	3.8221	49	0.6471	2.8448	γCH_3(wag) (29)
		60	1.4116	1.6166	61	0.075	28.6339	τCH_3 (37)
		81	7.9698	3.0385	81	2.2295	34.0105	γSO_2(wag) (32)
		89	0.4173	1.3121	88	6.1468	8.256	γCC (79)
	105	104	0.0768	0.6457	104	1.108	43.185	α CO (42) +βCCN (23)
		126	5.0908	1.9054	126	1.4992	49.5569	τ SO_2 (59)
	147	148	1.4896	3.4625	149	0.489	6.2906	α C N (48) + γCH (14)
	168	167	1.1743	0.6408	167	3.0434	2.3462	τCH_3 (47)
		175	0.2561	0.1019	176	1.1247	9.4554	β C N (43) + γCH (12)
	180	181	8.8129	0.9042	182	2.4597	0.4749	τCH_3 (57) +β C S (47)
	202	202	2.6661	1.7484	202	3.7682	22.807	τring 1 (31)
	210	209	3.255	2.8822	209	3.3481	31.7926	βNCC(16)
	233	232	2.0675	2.0205	233	1.2655	3.8238	τCH_2 (64)
		268	1.0732	2.2505	270	2.7694	94.8601	βCCC(35)+ γCS (39)
	285	286	0.8191	5.7751	286	4.9245	100.8237	νCC(34)+ βring (43)
	294	294	1.8401	7.8998	294	6.1272	3.9353	γring 1 (48)
	317	315	1.3048	1.5071	317	5.5577	6.1324	τring (16)+ βCCC (21)
		323	6.2537	2.9405	324	0.6027	58.5911	γCN (19)+ βring (13)
	335	336	0.8138	1.5803	337	0.2068	2.9776	τring(17)+ βNCH(13)
	394	393	0.2964	0.0868	393	3.1578	14.8264	γring 4 (57) + γCS (51)

(*contd.*)

Table 3 — Vibrational assignments of N3MP2MA using B3LYP/ 6-31 G(d,p) and B3LYP/6-311++G(d,p) (*contd.*)

νIR cm^{-1}	ν Raman cm^{-1}	B3LYP/6-31 G(d,p)			B3LYP/6-311++ G(d,p)			Assignments PED %
		ν cm^{-1}	IR intensity	Raman activity	ν cm^{-1}	IR intensity	Raman activity	
		396	1.8475	1.6939	398	7.7287	2.8079	δring 4 (56)
	408	410	13.0075	1.318	410	44.7903	25.435	τ ring (27) +γCH(18)
422		422	65.4564	1.2279	421	62.069	2.9317	β Ring (26) +γCN (16)
445	445	445	8.4924	2.2268	446	47.6609	37.1049	γCN (69), γring 4 (35)
451		450	4.8902	1.5518	453	6.8291	78.37	δNS (67), δring 4 (43)
503	502	503	11.4354	3.4959	503	65.6326	12.3087	τNC(19) +βCCO(27)
520	521	519	7.7688	5.7047	522	58.41	33.4099	βring (29)
525	525	525	32.0888	1.3	526	56.7045	18.127	γCH(18)+ γCN(19)
551		552	31.0963	1.5816	553	99.296	2.6844	νCS (65)
556	555	554	63.8334	6.627	555	4.0239	14.9607	γCO(57)+τNC(27)
	574	572	1.9833	0.4803	575	1.6002	1.1777	γNH (42)
589	589	588	23.6323	6.1348	590	59.5084	1.5838	νNS (54)
596	596	594	0.46	3.6917	595	1.8649	27.9628	γCC(32)
602		601	0.0295	3.1413	601	0.1381	20.8666	γCN(29)
640	641	639	8.0934	6.0681	642	48.8103	75.3617	βCCN(27)
662		661	32.7383	0.1409	663	97.3953	16.8839	βNCH(31)
679	680	680	8.3168	6.982	680	72.2857	18.3887	γCC(28)
	691	691	42.291	5.3785	691	12.4103	100.0471	γCH(26) + νCS (61)
723	723	723	39.4428	1.7902	724	13.4852	100.0755	βring(29)
727	728	727	65.2144	1.7938	729	65.5803	23.2009	γCH(86)+γCN(12)
731	731	731	9.7683	2.6868	732	23.3492	82.4465	γCH (54)
742	742	741	18.3154	1.3327	744	19.8855	1.8525	γCH(77) +νCC(29)
819	819	818	3.3046	3.3147	819	100.795	0.486	γCN(18)
830		830	0.0612	2.1532	831	7.5833	3.4495	γCC(34)+ τring(19)
846	845	845	20.6094	8.1487	847	12.7774	0.4689	γSO(59)
889	889	888	11.1296	4.2238	889	2.5251	0.0083	γSO(58)
899	900	898	2.7546	0.839	900	11.1144	36.9636	νCN(22)+ νCC(58)
902		901	2.3683	0.7292	903	2.9273	6.2589	γCN(21)
912	912	911	50.5692	3.2667	913	0.8458	12.3505	γCH(44)+ γCC(17)
936	936	935	0.4774	0.3138	939	1.3043	0.3144	γCH(37)+ βNCH(14)
941	941	940	2.7496	0.4127	942	14.4107	19.7162	νCC(51)+ νCN(33)
945		944	13.829	5.0212	947	8.6921	12.0767	γCO(22)+βCCH(13)
957	957	956	45.463	21.9119	958	67.6354	22.7942	γCH(36)+ βCCC(29)
962	962	962	2.329	7.246	963	65.8477	27.1624	νCC(53)+ τring(13)
	966	965	3.658	12.0872	967	30.4551	78.4173	βCCH(47)+ νCC(71)
998	998	995	2.7696	19.6873	998	6.9069	10.9907	βNCH(12)+ βring(29)
1003		1002	9.8864	25.4792	1004	73.643	5.5256	δSO (47)
1006	1006	1005	9.367	1.5392	1007	16.6447	14.2617	βCCH(23)+ βring(16)
1013	1013	1011	0.2219	0.854	1013	25.8592	3.2403	βNCH(26)+ βCCH(21)
1034	1035	1033	27.4018	9.0623	1035	17.6553	1.4674	νCC(56)+νCN(50)
1039	1039	1037	20.3717	2.1128	1040	36.6423	0.0824	βCCH(25)+νCC(62)
1046	1046	1045	9.3436	9.4411	1047	9.7405	14.8215	βCCH(39)
1059	1059	1058	6.5127	0.6059	1062	0.3786	7.7646	βCCH(33)+ νCC(65)
1090		1090	89.299	17.3751	1090	3.1263	2.2402	δCH (37)

(*contd.*)

Table 3 — Vibrational assignments of N3MP2MA using B3LYP/ 6-31 G(d,p) and B3LYP/6-311++G(d,p) (*contd.*)

νIR cm^{-1}	ν Raman cm^{-1}	B3LYP/6-31 G(d,p)			B3LYP/6-311++ G(d,p)			Assignments PED %
		ν cm^{-1}	IR intensity	Raman activity	ν cm^{-1}	IR intensity	Raman activity	
1092		1094	61.634	16.0601	1093	5.4886	5.5763	βCCH(22)+βCCO(21)
1107	1107	1106	70.1115	16.8634	1109	3.5652	22.1974	βCCH(43)+ βCCC(22)
1127	1127	1126	18.8062	4.7314	1126	55.1448	3.4751	βNCH(37)+ νCC(64)
1132	1132	1132	0.5189	5.5708	1132	2.3213	77.5854	νCC (86) + ν_sSO (74)
1150	1151	1150	1.5354	4.5438	1151	26.1408	1.787	βCCH(81)+νCN(44)
1164	1164	1164	82.8841	10.9827	1165	89.7926	22.4193	νCN(49)+ βCCC(16)
1190	1190	1189	56.3877	15.6335	1190	12.2909	10.4975	νCN(68)
1207	1207	1207	80.3972	8.5932	1208	10.5596	34.974	νCC(86) + βCCH(24)
1233	1232	1232	70.6303	26.3666	1233	15.9302	75.0234	νCN(71)
1262	1262	1261	14.6532	1.6887	1261	3.1785	12.0107	νCC(59) + βCCH(25)
1278	1277	1276	0.6862	0.3333	1278	3.1367	94.7824	νCC(67)
1289		1287	90.9551	2.0158	1288	9.9855	69.7929	νCC(66) + βCCC(22)
1301	1301	1299	8.0198	3.188	1300	0.5534	93.2999	νCN(58)+ βCCC(21)
1310	1310	1309	41.2614	8.2916	1310	28.9396	23.0414	νCN(69)
	1329	1327	2.2336	14.7836	1328	5.0129	51.8361	νCC (73)+ βHCH(11)
1337	1337	1337	9.0714	47.7988	1339	37.1603	0.2595	νCC(47) + βCCC(21)
1345		1345	19.1518	52.0676	1345	4.1165	1.9531	νCC(59) + βCCH(32)
1368	1368	1365	0.0806	39.687	1366	28.0741	42.2002	βHCH(51) + ν_aSO(87)
1409	1409	1410	10.3815	10.0816	1410	6.1946	35.0286	βHCH(54) + βCCH(33)
1413	1412	1413	57.7265	20.606	1414	76.0601	7.5005	βCCH(39)
1416		1414	12.7868	1.1072	1415	12.3309	92.4359	βCCH(47) + νCC(62)
1423	1423	1421	7.1162	17.7439	1423	57.0678	20.7619	βCCH(23) + νCC(76)
1429	1430	1428	11.9464	14.7082	1430	77.7866	20.5928	βHCH(43) + βCCH(32)
1435		1434	1.9026	26.5689	1433	28.0787	86.5277	νCC(65)
1443	1445	1444	3.6992	8.0519	1445	12.6067	10.8981	νCN(91)
1448		1446	2.5914	12.7465	1447	7.6807	22.0221	νCC(86) + βring(23)
1460		1458	41.1638	16.3582	1460	98.4504	1.8573	νCC(77) +βCCH(24)
1470	1469	1469	100.3613	2.3101	1470	17.8983	5.1707	$\beta_s CH_3$ (63)
1539	1538	1539	1.4384	65.0289	1540	4.8175	4.0939	$\beta_s CH_2$ (81)
1556	1557	1558	0.5773	41.8008	1558	26.3153	0.0951	βCCH(47)
1560	1560	1561	0.0518	12.692	1560	98.9762	15.3904	$\beta_s CH_3$ (76)
1568	1567	1567	0.3983	81.6849	1568	18.3875	2.3194	β NH (73)
1580	1579	1580	6.8933	26.6165	1580	0.1214	6.3774	$\beta_{as} CH_3$ (45)
1623	1623	1624	98.3791	4.3365	1623	100.5495	1.2147	νC=O(61)
2890	2889	2885	9.0874	64.0933	2889	25.5216	9.7633	ν CH(94)
2897	2896	2895	6.9486	69.4915	2897	25.7657	1.1956	ν CH(97)
2905	2906	2907	7.3552	63.7192	2909	0.7819	4.3273	ν_s CH(96)
2931	2932	2933	15.9927	95.3226	2933	2.2757	3.157	ν_s CH(97)
2973	2973	2973	17.2072	56.6483	2974	13.5981	1.2742	ν_s CH(99)
2987	2988	2988	13.718	34.571	2988	9.0411	3.5146	ν_s CH(98)
3005	3002	3003	7.9339	79.5636	3005	67.3939	2.0447	ν CH(99)
3025	3027	3026	0.6815	57.4701	3028	1.6905	0.4447	ν_s CH(97)
3030		3029	4.0915	30.231	3030	38.9254	0.8925	ν CH(98)
3036	3036	3034	1.2296	55.0435	3037	10.398	0.2756	ν_{as}CH(99)
3043	3041	3042	12.5821	73.3245	3043	45.6788	0.7284	ν CH(99)
3046	3047	3046	10.329	63.6044	3046	11.5112	0.2724	ν_{as}CH(97)

(*contd.*)

Table 3 — Vibrational assignments of N3MP2MA using B3LYP/ 6-31 G(d,p) and B3LYP/6-311++G(d,p) (*contd.*)

νIR cm^{-1}	ν Raman cm^{-1}	B3LYP/6-31 G(d,p)			B3LYP/6-311++ G(d,p)			Assignments PED %
		ν cm^{-1}	IR intensity	Raman activity	ν cm^{-1}	IR intensity	Raman activity	
3051	3050	3049	10.0223	100.4083	3050	27.6843	0.5952	ν_{as}CH(98)
3056	3055	3054	11.7925	83.6734	3054	74.1809	0.5798	ν_{as}CH(99)
3067		3066	3.8578	97.0023	3068	57.4052	1.8609	ν_{as}CH(98)
3079	3080	3079	10.0639	51.7703	3081	51.8694	0.8699	ν_{as}CH(99)
3103	3104	3102	1.8725	64.7029	3106	52.154	1.3111	ν_{as}CH(98)
3466	3468	3467	17.2339	29.3562	3471	74.4162	2.3423	ν NH(98)

Table 4 — The calculated μ, α and βcomponents of N3MP2MA

Parameters	B3LYP/6-31G(d,p)	B3LYP/6-311++G(d,p)	Parameters	B3LYP/6-31G(d,p)	B3LYP/6-311++G(d,p)
μ_x	-7.7650	-7.4156	β_{xxx}	736.656	565.678
μ_y	-2.5181	-2.9167	β_{xxy}	545.425	-58.574
μ_z	0.0528	-0.2380	β_{xyy}	-85.053	43.012
μ	8.1633	7.7377	β_{yyy}	-19.476	-8.431
α_{xx}	438.157	311.741	β_{xxz}	33.196	53.674
α_{xy}	-2.539	-4.117	β_{xyz}	-3.877	-5.565
α_{yy}	237.636	204.792	β_{yyz}	7.352	-21.675
α_{xz}	6.942	6.750	β_{xzz}	-8.105	6.648
α_{yz}	-7.557	-13.043	β_{yzz}	-4.353	0.546
α_{zz}	73.712	88.437	β_{zzz}	0.611	0.535
α_{tot}	142.949	156.935	β_{tot}(esu)	1.21×10^{-30}	1.26×10^{-30}
Δα	397.386	430.293			

Table 3 that the predicted vibrational bands agree well with the observed ones.

4.2.4 SO_2 vibrations

The symmetric and asymmetric SO_2 stretching vibrations[31] occur in the region 1125-1150 cm^{-1} and 1295-1350 cm^{-1}. It is stated that, in our present compound, the SO_2 symmetric and asymmetric stretching vibrations occur at 1132 cm^{-1} and at 1368 cm^{-1}, respectively. The experimental FTIR and FT Raman shows band in the these regions. The SO_2 in plane and out of plane bending vibrations for our title compound are predicted at 394, 268 and 180 cm^{-1}, respectively.

5 Molecular Properties

5.1 NLO properties

Many organic molecules that contains conjugated π electron are characterized and hyperpolarizabilities have been analyzed by means of vibrational spectroscopy[32,33]. Both the B3LYP/6-31G(d,p) and B3LYP/6-311++G(d,p) method has been used for the prediction of first order hyperpolarizability (β) of the title compound. The tensor components of the static first order hyperpolarizability (β) were analytically calculated by using the same method as mentioned above. From the computed tensorial components, β is calculated for the title compound by taking into account the Kleimman symmetry relations and the square norm of the cartesian expression for the β tensor[34]. The first order hyperpolarizability (β) of this novel molecular system and the related properties (α_0 and Δα) of N3MP2MA were calculated, based on the finite field approach. The complete equation for calculating the magnitude of the total static dipole moment μ, the mean polarizability α_0, the anisotropy of the polarizability Δα, and the mean first order hyperpolarizability β, using the x, y, z components are defined as follow:

$$\mu = [\mu^2_x + \mu^2_y + \mu^2_z]^{1/2}$$

$$\beta = [\beta^2_x + \beta^2_y + \beta^2_z]^{1/2}$$

$$\alpha = \frac{\alpha_{xx} + \alpha_{yy} + \alpha_{zz}}{3}$$

$$\Delta\alpha = 2^{-1/2} [(\alpha_{xx} - \alpha_{yy})^2 + (\alpha_{yy} - \alpha_{zz})^2 + (\alpha_{zz} - \alpha_{xx})^2 + 6\alpha^2_{xx}]^{1/2}$$

where

$$\beta_x = \beta_{xxx} + \beta_{xyy} + \beta_{xzz}$$

$$\beta_y = \beta_{yyy} + \beta_{xxy} + \beta_{yzz}$$

$$\beta_z = \beta_{zzz} + \beta_{xxz} + \beta_{yyz}$$

The components of polarizability and the first order hyperpolarizability of the title compound can be seen in Table 4. The calculated value of first hyperpolarizability shows that N3MP2MA might have the NLO properties.

5.2 MEP

The molecular electrostatic potential (MEP) has been used extensively for the analysis of molecular interactions, including chemical reactions, hydrogen bonding, salvation processes and bio molecular recognition interactions. These are also types of regions that are known to be susceptible to electrophilic attack, which further confirms that minima in the potential are useful for characterizing sites for electrophilic attack. It should be noted that most neutral molecules have regions of negative potential and thereby also associated V_{min}. However, for non polar molecules held together by σ-bonds and alkanes the magnitudes of the V_{min} are often small, indicating low degrees of electrophilic susceptibility. It should therefore be stressed that the existence of minima should not be used by itself to identify sites for electrophilic attack but that also the magnitudes of the V_{min} need to be considered.

The electrostatic potential and the V_{min} are not only useful for the prediction of interaction with protons but also with other electrophiles, and in particular for interactions with hydrogen bond donors. However, the positive exchange-repulsion energy is largely cancelled by the negative energy contributions from polarization and charge transfer, which is the reason that the electrostatic interaction energy is reasonably close to the total interaction energy. This is a general observation that the position and magnitude of V_{min} can be used to characterize lone pairs in molecules. It can be noted that the existence of the lone pairs is not as easily deduced from an analysis of the electron density. Other molecular regions that generally exhibit minima in the potential are π-regions, including multiple bonds and aromatic groups. To predict regions more susceptible to approximation of either electrophiles or nucleophiles, MESP was calculated at the B3LYP/6-311++G(d,p) and is shown in Fig. 5. The red indicates negative regions, blue indicates positive regions, while green appears over zero electrostatic potential regions. It is accepted that the negative (red) and the positive (blue) potential regions in the mapped MESP represent regions susceptible to approach electrophilic molecules or nucleophilic molecules, respectively. The contour map provides a simple way to predict how different geometries could interact and is shown in Fig. 6.

5.3 NBO

The natural bond orbital (NBO) calculations were performed using NBO 3.1 program[35] as implemented

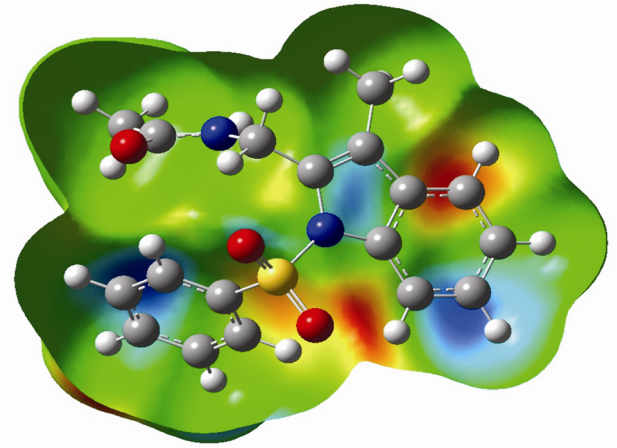

Fig. 5 — Molecular electrostatic potential of N3MP2MA

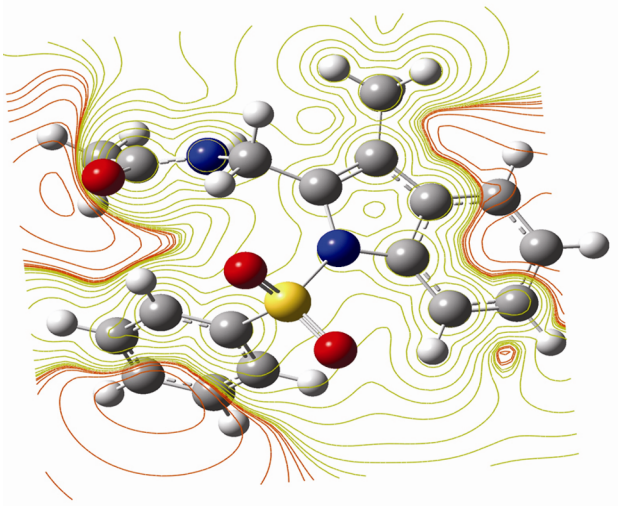

Fig. 6 — The contour map of electrostatic potential of the total density of N3MP2MA

in the Gaussian03 package at the DFT/B3LYP level in order to understand various second-order interactions between the filled orbital of one subsystem and vacant orbital of another subsystem, which is a measure of the intermolecular delocalization or hyper conjugation. NBO analysis provides the most accurate possible 'natural Lewis structure' picture of '*j*' because all orbital details are mathematically chosen to include the highest possible percentage of the electron density. A useful aspect of the NBO method is that it gives information about interactions of both filled and virtual orbital spaces that could enhance the analysis of intra and inter molecular interactions. The second-order Fock-matrix was carried out to evaluate the donor–acceptor interactions in the NBO basis. The interactions result in a loss of occupancy from the localized NBO of the idealized Lewis structure into

an empty non-Lewis orbital. For each donor (*i*) and acceptor (*j*) the stabilization energy (E2) associated with the delocalization $i \rightarrow j$ is determined as $E^{(2)} = \Delta E_{ij} = q_i \frac{F(i,j)^2}{\varepsilon_i - \varepsilon_j}$ where q_i is the donor orbital occupancy, ε_i and ε_j are diagonal elements and $F(i, j)$ is the off diagonal NBO Fock matrix element. In Table 5 the perturbation energies of significant donor–acceptor interactions are presented. The larger the $E(2)$ value, the intensive is the interaction between electron donors and electron acceptors. In N3MP2MA, the interactions between the bonding C18-C19 and the corresponding antibonding C20-C21, C22-C23 have the highest $E(2)$ value around 319.98, 251.74 kcal/Mol.

The NBO analysis also describes the bonding in terms of the natural hybrid orbital π*C20-C21, which occupy a higher energy orbital (1.97730 a.u.) with considerable p-character (64.44%) and the other occupy π*C18-C19 a lower energy orbital (1.97231a.u.) with p-character (62.61%). The NBO analysis also describes the bonding in terms of the natural hybrid orbital LP(1)N4, which occupy a higher energy orbital (1.71093a.u.) with considerable p-character (99.98%) and the other LP(1)N6 occupy a lower energy orbital (1.71303) with p-character (58.04%). Thus, a very close to pure p-type bonding orbital participates in the electron donation to the π*(C18–C19) orbital for π*(C18–C19)→ π*(C20–C21) and π*(C18–C19)→ π*(C22–C23). The results are tabulated in Table 6.

5.4 Natural atomic charges

The computation of the reactive atomic charges plays an important role in the application of quantum mechanical calculations for the molecular system. Mulliken population analysis provides a partitioning of either a total charge density or an orbital density In order to determine the electron population of each atom of the title molecule, the natural atomic charges of N3MP2MA calculated by DFT/B3LYP method using 6-31G(d,p) and 6-311++G(d,p)basis set. Illustration of atomic charges plotted graphically and structurally are shown in Figs 7 and 8. For Mulliken

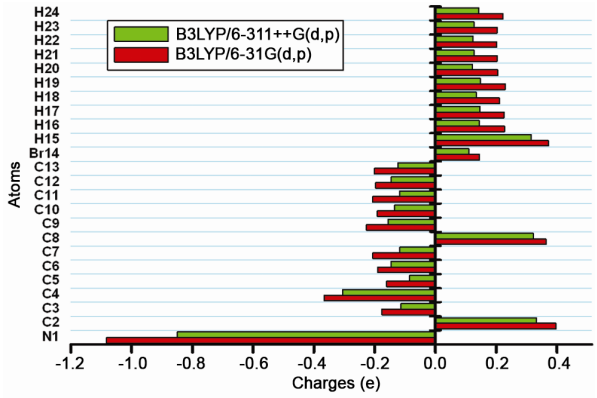

Fig. 7 — Histogram of calculated Mullikan atomic charges of N3MP2MA

Table 5 — NBO analysis of N3MP2MA

Donor	Acceptor	$E^{(2)}$KJ/mol[a]	E(j)-E(i)[b] a.u.	F(i,j)[c] a.u.
π*C9-C14	π*C7-C8	33.93	0.26	0.088
π*C20-C21	π*C18-C19	25.40	0.29	0.078
LP(1) N4	π*C1-O13	62.92	0.30	0.123
LP(1) N6	π*C9-C14	68.11	0.27	0.126
π*C7-C8	π*C9-C14	76.26	0.05	0.087
π*C18-C19	π*C20-C21	319.98	0.01	0.092
π*C18-C19	π*C22-C23	251.74	0.01	0.086

[a] E(2) means energy of hyperconjugative interactions (stabilization energy in kJ/mol).
[b] Energy difference (a.u.) between donor and acceptor i and j NBO orbitals.
[c] F(i,j) is the Fock matrix elements (a.u.) between i and j NBO orbitals.

Table 6 — NBO results showing the formation of Lewis and non-Lewis orbitals

Bond(A-B)	ED/energy	EDA%	EDB%	NBO	s%	p%
π*C9-C14	1.94882	50.68	49.32	0.7119(sp1.96)C+0.7023(sp1.85)C	33.75	66.21
π*C20-C21	1.97730	50.01	49.99	0.7072(sp1.81)C+0.7070(sp1.82)C	35.52	64.44
π*C18-C19	1.97231	51.11	48.89	0.7149(sp1.64)C+0.6992(sp1.85)C	37.85	62.11
LP(1)N4	1.71093	-	-	P1.00	0.01	99.98
LP(1)N6	1.71303	-	-	P1.00	41.93	58.04

charge distribution, the GaussView adopts the follow colors scheme: bright red for more negative charge and bright green for a more positive charge. The red hues illustrate negative charges while green hues expose positive charges. The charge distribution of the compound shows that carbon atom (C_8) attached with nitrogen atoms have negative charges. All the hydrogen atoms have positive Mulliken charges. The atom C_1 has the highest Mulliken charge (0.581124) when compared to other atoms. The nitrogen (N_4) atoms are much more negative charge than the other atoms. The smallest Mulliken charge value (–0.514935) was obtained for O3 atom. The Mulliken charge distribution and the MESP informations are concordant. The total atomic charges of N3MP2MA using B3LYP/6-31G(d,p) and B3LYP/6-311++G(d,p) methods are listed in Table 7.

5.5 Global and local reactivity descriptors

The Highest Occupied Molecular Orbitals (HOMOs) and Lowest–Lying Unoccupied Molecular Orbitals (LUMOs) are named as Frontier molecular orbitals (FMOs). The energy gap between the HOMOs and LUMOs is the critical parameters in determining molecular electrical transport properties helps in the measure of electron conductivity. To understand the bonding feature of the title molecule, the plot of the Frontier orbitals, the highest occupied molecular orbital HOMO and lowest unoccupied molecular orbital LUMO are shown in Fig. 9. The HOMO shows that the charge density localized mainly on carbonyl and amine group where as LUMO is localized on ring system. Gauss-Sum 2.2 Program[36] has been used to calculate group contributions to the molecular orbitals and prepare the density of the state (DOS) as shown in Fig. 10. The DOS spectra were created by convoluting the molecular orbital

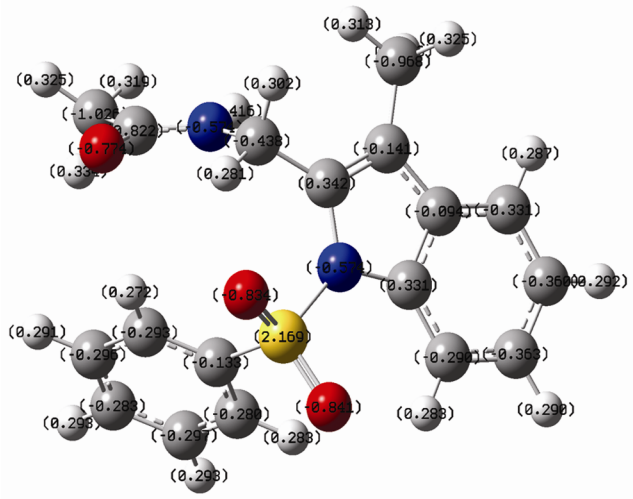

Fig. 8 — Structural charge distribution of N3MP2MA

Table 7 — Mullikan atomic charges table of N3MP2MA

Atom	B3LYP/6-31G(d,p)	B3LYP/6-311++G(d,p)	Atom	B3LYP/6-31G(d,p)	B3LYP/6-311++G(d,p)
C_1	0.581124	0.312256	C_{22}	-0.089444	-0.039712
C_2	-0.394340	0.489578	C_{23}	-0.070396	0.081619
O_3	-0.514935	-0.134178	C_{24}	-0.386651	0.309917
N_4	-0.520608	-0.471992	H_{25}	0.095712	0.085780
C_5	-0.105693	0.090290	H_{26}	0.149689	0.109117
N_6	-0.783902	-0.613178	H_{27}	0.138568	0.109336
C_7	0.248198	-0.208937	H_{28}	0.255119	0.211227
C_8	0.025392	-0.019057	H_{29}	0.133648	0.131918
C_9	0.051427	-0.011121	H_{30}	0.195815	0.211800
C_{10}	-0.143542	0.106032	H_{31}	0.077375	0.014082
C_{11}	0.090237	-0.051535	H_{32}	0.076998	0.013430
C_{12}	-0.110895	-0.133594	H_{33}	0.084668	0.110462
C_{13}	-0.088615	-0.030063	H_{34}	0.132514	0.189344
C_{14}	0.289769	0.262391	H=	0.174585	0.048675
S_{15}	1.292028	-1.109851	H_{36}	0.113153	0.098476
O_{16}	-0.530636	-0.509806	H_{37}	0.093662	0.139764
O_{17}	-0.520791	0.425173	H=	0.095432	0.112384
C_{18}	-0.181804	-0.110843	H=	0.124755	0.123754
C_{19}	-0.081146	-0.074532	H=	0.111922	0.098465
C_{20}	-0.098461	0.038343	H=	0.134952	0.129746
C_{21}	-0.075325	-0.040309	H_{42}	0.112555	0.089874

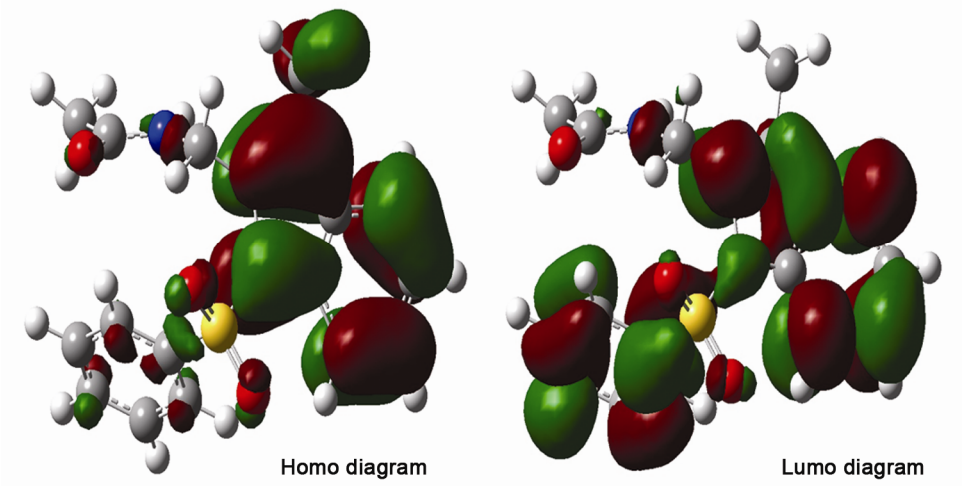

Fig. 9 — Frontier molecular orbital N3MP2MA

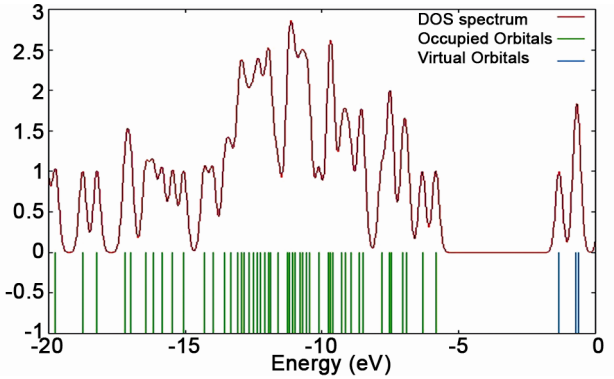

Fig. 10 — DOS spectrum of N3MP2MA

information with GAUSSIAN curves of the unit height.

By using HOMO and LUMO energy values for a molecule, the global chemical reactivity descriptors of molecules such as hardness, chemical potential, softness, electronegativity and electrophilicity index as well as local reactivity have been defined[37-41]. Pauling introduced the concept of electronegativity as the power of an atom in a molecule to attract electrons to it. Hardness (η), chemical potential (μ) and electronegativity (χ) and softness are defined follows.

$$\eta = 1/2\ (\partial^2 E/\partial N^2)\ V(r) = 1/2\ (\partial\mu/\partial N)\ V(r)$$

$$\mu = (\partial E/\partial N)\ V(r)$$

$$\chi = -\mu = -(\partial E/\partial N)\ V(r)$$

where E and $V(r)$ are electronic energy and external potential of an N-electron system, respectively. Softness is a property of a molecule that measures the extent of chemical reactivity. It is the reciprocal of hardness:

$$S = 1/\eta$$

Using Koopman's theorem for closed-shell molecules, η, μ and χ can be defined as:

$$\eta=(I-A)/2 \qquad \mu=-(I+A)/2 \qquad \chi=(I+A)/2$$

where A and I are the ionization potential and electron affinity of the molecules, respectively. The ionization energy and electron affinity can be expressed through HOMO and LUMO orbital energies as $I = -E_{HOMO}$ and $A = -E_{LUMO}$. Electron affinity refers to the capability of a ligand to accept precisely one electron from a donor. The ionization potential calculated by B3LYP/6-31G(d,p) and B3LYP/6-311++G(d,p) methods for N3MP2MA is 5.8255eV and 5.8723 eV, respectively. Considering the chemical hardness, large HOMO–LUMO gap means a hard molecule and small HOMO–LUMO gap means a soft molecule. One can also relate the stability of the molecule to hardness, which means that the molecule with least HOMO–LUMO gap means it, is more reactive. Recently Parr *et al.*[37] has defined a new descriptor to quantify the global electrophilic power of the molecule as an electrophilicity index (ω), which defines a quantitative classification of the global electrophilic nature of a molecule Parr *et al.*[37] have proposed electrophilicity index (ω) as a measure of energy lowering due to maximal electron flow between donor and acceptor. They defined electrophilicity index (ω) as follows:

$$\omega=\mu^2/2$$

Using the above equations, the chemical potential, hardness and electrophilicity index have been

calculated for N3MP2MA and their values are shown in Table 8. The usefulness of this new reactivity quantity has been recently demonstrated in understanding the toxicity of various pollutants in terms of their reactivity and site selectivity[42-44]. The calculated value of electrophilicity index describes the biological activity of N3MP2MA.

5.6 Temperature dependence of thermodynamic properties

The statistical thermodynamics, like the standard thermodynamic functions such as heat capacity, entropy and enthalpy were calculated using perl script THERMO.PL[45] and are listed in Table 9. As observed from the Table 9, the values of C_P, H and S all increase with the increase of temperature from 100 to 1000 K, which is attributed to the enhancement of the molecular vibration as the temperature increases. The correlation equations between heat capacity (C°pm), entropy(S°_m), enthalpy (H°_m) changes and temperatures were fitted by quadratic formulas and the corresponding fitting factors (R^2) for these thermodynamic properties are 0.9999, 0.9998 and 0.9998, respectively. The corresponding fitting equations are as follows and the correlation graphs of those shown in Fig. 11.

Table 8 — Molecular properties of N3MP2MA

Molecular properties	B3LYP		Molecular properties	B3LYP	
	6-31G(d,p)	6-311++G(d,p)		6-31G(d,p)	6-311++G(d,p)
E_{HOMO}(eV)	-5.8255	-5.8723	Chemical hardness(η)	4.5353	4.0442
E_{LUMO}(eV)	-1.2846	-1.8281	Softness(S)	0.2205	0.2472
$E_{HOMO-LUMO}$ gap(eV)	-4.5353	-4.0442	Chemical potential(μ)	-3.5550	-3.8502
Ionisation potential(I)eV	5.8255	5.8723	Electronegativity (χ)	3.5550	3.8502
Electron affinity(A)eV	1.2846	1.8281	Electrophilicity index (ω)	6.3190	7.4129

Table 9 — Thermo dynamical properties of N3MP2MA

T (K)	*S* (J/mol.K)		*Cp* (J/mol.K)		*ddH* (kJ/mol)	
100	406.655	418.24	153.77	156.55	9.83	9.92
200	542.514	557.97	253.82	258.48	30.39	30.66
298.15	661.456	680.35	355.07	361.47	60.53	61.07
300	663.634	682.54	356.97	363.41	61.20	61.74
400	778.851	801.04	455.05	463.25	102.27	103.17
500	888.556	913.87	538.80	548.51	152.55	153.89
600	991.979	1020.24	607.00	617.94	210.49	212.34
700	1088.85	1119.87	662.24	674.18	274.63	277.04
800	1179.42	1213.31	707.53	720.28	343.82	346.84
900	1264.14	1300.11	745.16	758.59	417.17	420.84
1000	1343.49	1381.76	776.81	790.81	494.01	498.35

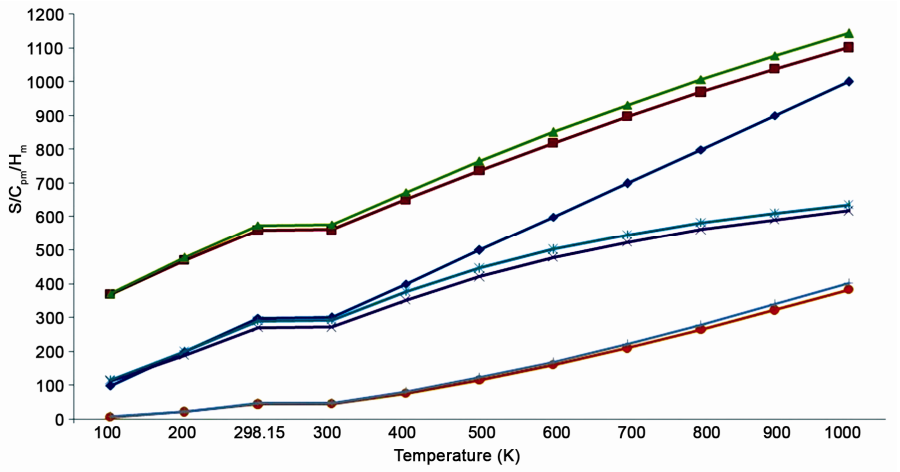

Fig. 11 — Thermodynamical properties of N3MP2MA by B3LYP/6-31G(d,p) and B3LYP/6-311++G(d,p)

$S^{o}m = 240.03433 + 0.7328\ T - 1.79433\times10^{-4}\ T^{2}$ (R^2 = 0.9999)

$C^{o}pm = 15.26587 + 0.65639\ T - 2.82786\times10^{-4}\ T^{2}$ (R^2 = 0.9998)

$H^{o}_{m} = -7.65942 + 0.08696\ T + 1.73344\times10^{-4}\ T^{2}$ (R^2 = 0.9998)

All the thermodynamic data provide helpful information to further study of the title compounds. They compute the other thermodynamic energies according to the relationship of thermodynamic functions and estimate directions of chemical reactions according to the second law of thermodynamics in thermo chemical field. All thermodynamic calculations were done in gas phase and they could not be used in solution.

6 Conclusions

A complete structural, thermodynamic, first-order hyperpolarizability, Mulliken population analysis, vibrational and electronic investigations of N3MP2MA have been carried out with FTIR and FT-Raman spectroscopic technique along with DFT/B3LYP method with different basis sets. The gas phase structure and conformational properties of N3MP2MA and its conformers were determined by quantum chemical calculations. It is found that molecule has three conformations. The equilibrium geometries and harmonic frequencies of N3MP2MA was determined and analyzed at the DFT level utilizing 6-31G(d,p) and 6-311++G(d,p) basis set, giving allowance for the lone pairs through diffuse functions. The difference between observed and calculated wavenumber values of the most of the fundamental modes is very small. Any discrepancy noted between the observed and the calculated vibrational band assignments may be due to the fact that the calculations have been actually done on a single molecule in the gaseous state contrary to the experimental values recorded in the presence of intermolecular interactions. The various intramolecular interactions that is responsible for the stabilization of the molecule was revealed by natural bond orbital analysis. The lowering of HOMO and LUMO energy gap clearly explicates the charge transfer interactions taking place within the molecule.

References

1 Singh U P, Sarma B K, Mishra P K, & Ray A B, *Fol Microbiol*, 45 (2000) 173.

2 Andreani A, Granaiola M, Leoni A, Locatelli A, Morigi R, Rambaldi M, Giorgi G, Salvini L & Garaliene V, *Anticancer Drug Des*, 16 (2001) 167.

3 Quetin-Leclercq J, *J Pharm Belg*, 49 (1994) 181.

4 Mukhopadhyay S, Handy G A, Funayama S & Cordell G A, *J Nat Prod*, 44 (1981) 696.

5 Taylor D L, Ahmed P S, Chambers P, Tyms A S, Bedard J, Duchaine J, Falardeau G, Lavallee J F, Brown W, Rando R F & Bowlin T, *Antivir Chem Chemother*, 10 (1999) 79.

6 Williams T M, Ciccarone T M, Tough S C M, Rooney C S, Balani S K, Condra J H, Emini E A, Goldman M E, Greenlee W J & Kauffman L R, *J Med Chem*, 36 (1993) 1291.

7 Sivaraman J, Subramanian K, Velmurugan D, Subramanian E & Seetharaman J, *J Mol Struct*, 385 (1996) 123.

8 Thenmozhi S, Pandi A S, Dhayalan V & Mohanakrishnan A K, *Acta Cryst*, 65 (2009) 1020.

9 Frisch M J, Trucks G W, Schlegel H B, Scuseria G E, Robb M A, Cheeseman J R, Montgomery J A, Vreven T, Kudin K N, Burant J C, Millam J M, Iyengar S S, Tomasi J, Barone V, Mennucci B, Cossi M, Scalmani G, Rega N, Petersson G A, Nakatsuji H, Hada M, Ehara M, Toyota K, Fukuda R, Hasegawa J, Ishida M, Nakajima T, Honda Y, Kitao O, Nakai H, Klene M, Li X, Knox J E, Hratchian H P, Cross J B, Bakken V, Adamo C, Jaramillo J, Gomperts R, Stratmann R E, Yazyev O, Austin A J, Cammi R, Pomelli C, Ochterski J W, Ayala P Y, Morokuma K, Voth G A, Salvador P, Dannenberg J J, Zakrzewski V G, Dapprich S, Daniels A D, Strain M C, Farkas O, Malick D K, Rabuck A D, Raghavachari K, Foresman J B, Ortiz J V, Cui Q, Baboul AG, Clifford S, Cioslowski J, Stefanov B B, Liu G, Liashenko A, Piskorz P, Komaromi I, Martin R L, Fox D J, Keith T, Al-Laham M A, Peng C Y, Nanayakkara A, Challacombe M, Gill P M W, Johnson B, Chen W, Wong M W, Gonzalez C & Pople J A, Gaussian 03W Program, Gaussian Inc, Wallingford, CT, 2004.

10 Karabacak M, Postalcilar E & Cinar M, *Spectrochim Acta Part A*, 85 (2012) 261.

11 Pulay P, Fogarasi G, Pongor G, Boggs J E & Vargha A, *J Am Chem Soc* ,105 (1983) 7037.

12 Rauhut G & Pulay P, *J Phys Chem*, 99 (1995) 3093.

13 Fogarasi G, Pulay P & Durig J R, *Vibrational spectra and structure*, (Elsevier, Amsterdam), 1985.

14 Fogarasi G, Zhou X, Taylor P W & Pulay P, *J Am Chem Soc*, 114 (1992) 8191.

15 Sundius T, *J Mol Struct*, 218 (1990) 321.

16 Sundius T, *Vib Spectrosc*, 29 (2002) 89.

17 MOLVIB (V70): *Calculation of harmonic force fields and vibrational modes of molecules*, QCPE Program No 807, 2002.

18 Frisch A, Nielson A B & Holder A J, Gaussview users manual), Gaussian Inc, Pittsburgh, PA), 2000.

19 Sajan D, Ravindra H J, Misra N & Joe I H, *Vib Spectrosc*, 54 (2010) 72.

20 Thilagavathi G & Arivazhagan M, *Spectrochim Acta*, 79 (2010) 389.

21 Gunasekaran S, Seshadri S, Muthu S, Kumaresan S & Arunbalaji R, *Spectrochim Acta A*, 70 (2008) 550.

22 Puviarasan N, Arjunan V & Mohan S, *Turk J Chem*, 26 (2002) 323.

23 Varsanyi G, *Assignments for vibrational spectra of seven hundred benzene derivatives*, (Academic Kiaclo, Budapest), 1973.

24 Abkowicz-Bienko A J, Latajka Z, Bienko D C & Michalska D, *Chem Phys*, 250 (1999) 123.
25 Krishnakumar V & Balachandran V, *Spectrochim Acta*, 61 **(**2005) 1811.
26 Xavier J, Raja S, William S & Gunasekaran S, *Orient J Chem*, 10 **(**1994) 3.
27 Gunasekaran S, Natarajan R K, Rathika R & Syamala D, *Ind J Phys*, 79 (2005) 509.
28 Gunasekaran S, Kumaresan P, Manoharan K & Mohan S, *Asian J Chem*, 6 (1994) 821.
29 Silverstein M, Basseler G C, Morill C, *Spectrometric identification of organic compounds*, (Wiley, New York), 1981.
30 Sing N P & Yadav R A, *Ind J Phys*, 75 (2001) 347.
31 Karabacak M, Cinar M, Kurt M, Poiyamozhi A & Sundaraganesan N, *Spectrochim Acta Part A*, 117 (2014) 234.
32 Thomson H W & Torkington P, *J Chem Soc*, 171 (1945) 640.
33 Glendening E D, Badenhoop J K, Reed A E, Carpenter J E, Bohmann J A, Morales C M & Weinhold F, NBO-50, Theoretical Chemistry Institute, University of Wisconsin, Madison, 2001.
34 Reed A E, Curtiss L A & Weinhold F, *Chem Rev*, 88 (1988) 899.
35 Glendening E D, Reed A E, Carpenter J E & Weinhold F, NBO Version 31, TCI,
36 University of Wisconsin: Madison, 1998.
37 Boyle N M O, Tenderholt A L & Langer K M, *J Comput Chem*, 29 (2008) 839.
38 Parr R G, Szentpaly L & Liu S, *J Am Chem Soc*, 121 (1999) 1922.
39 Chattaraj P K, Maiti B & Sarkar U, *J Phys Chem A*, 107 (2003) 4973.
40 Parr R G, Donnelly R A, Levy M & Palke W E, *J Chem Phys*, 68 (1978) 3801.
41 Parr R G & Pearson R G, *J Am Chem Soc*, 105 (1983) 7512.
42 Parr R G & Chattraj P K, *J Am Chem Soc*, 113 (1991) 1854.
43 Parthasarathi R, Padmanabhan J, Elango M, Subramanian V & Chattaraj P, *Chem Phys Lett*, 394 (2004) 225.
44 Parthasarathi R, Padmanabhan J, Subramanian V, Maiti B & Chattaraj P, *Curr Sci*, 86 (2004) 535.
45 Parthasarathi R, Padmanabhan J, Subramanian V, Sarkar U, Maiti B & Chattaraj P, *Internet Electron J Mol Des*, 2 (2003) 798.
46 Irikura K K, THERMOPERL Script, *National Institute of Standards and Technology*, 2002.